INTERNATIONAL JOURNAL OF CLIMATOLOGY
Int. J. Climatol. **30**: 72–88 (2010)
Published online 2 March 2009 in Wiley InterScience
(www.interscience.wiley.com) DOI: 10.1002/joc.1873

RMetS
Royal Meteorological Society

An analytical framework for estimating the urban effect on climate

Benjamin Lamptey*†
National Center for Atmospheric Research, Research Applications Laboratory, PO Box 3000 Boulder, CO 80307-3000, USA

ABSTRACT: The surface energy budget has been used to illustrate the influence of urban landscape on both global and regional climate. This was done using empirical as well as remotely sensed data of components of the surface energy equation.

At the global scale, the urban land cover has the least impact on the sensible and latent heat fluxes compared to the other land cover types. Replacing the urban land cover with vegetation did not result in a significant change to the proportionate values of the turbulent fluxes originally due to vegetation. The least impact of current urbanization on the global climate in terms of radiation and surface fluxes is because the urban land cover has the smallest fraction of all the land cover types.

The relative importance of the urban landscape at the regional scale was illustrated using the example of Chester County and surroundings near Philadelphia, Pennsylvania, in the USA. The urban effect becomes more important as the fraction of urban land cover to the total increases. This is illustrated by computing turbulent fluxes for 1987, 1988, 1991, 1993 and 1996 over the Chester County area. Urbanization in Chester County and surrounding areas increased from 11% in 1987 to 19% in 1996. In 1996, urban land cover produced the largest proportionate sensible (21.4 Wm^{-2}) and latent (14.2 Wm^{-2}) heat fluxes during winter. During the 1996 summer, urban and vegetation land cover produced the largest proportionate sensible heat (59.2 Wm^{-2}) while urban land cover produced the second largest proportionate latent heat flux (39.5 Wm^{-2}). The implications of this simple analytical study point to the need to account for the urban landscape particularly in regional studies.

KEY WORDS global climate models; mesoscale atmospheric models; urbanization; land cover change; surface energy balance

Received 31 January 2008; Revised 15 November 2008; Accepted 13 January 2009

1. Introduction

The impact of land use and land cover on the climate and climate change is well known (e.g. Chase *et al*., 2000; Voldoire and Royer, 2004; Molders and Olson, 2004; Bottyan *et al*., 2005; Miller *et al*., 2005; Lamptey *et al*., 2005a,b). An issue of current interest is the improved representation of urban land cover in atmospheric models. One of the needs for the improved representation of urban land cover in atmospheric models is to better capture the urban heat island (UHI), which is the most well known atmospheric effect of towns. Another need for the improved representation of the urban land cover is the fact that urban landscapes modify the original physical processes that govern any natural land surface [i.e. surface energy budget (SEB)] and also add new biogeophysical and biogeochemical processes into the land surface-atmosphere, such as the storage heat flux, canyon effect and anthropogenic heat flux (e.g. Jin and Shepherd, 2005). The UHI effect has economic consequences as well as an impact on health (e.g. Masson, 2006). The study of urban climate is important to first ensure a pleasant and healthy environment for urban dwellers, and second, to see that the effects of urbanization do not have harmful repercussions on large-scale (even planetary) climates (e.g. Oke, 1987). The ideal approach to quantify the impact of urbanization on the climate of a geographical region is to have measurements of the climatic variables before the region became urbanized and compare these to the measurements after urbanization has occurred. This approach is preferable to the current one, where the difference between the climatic variables taken in an urban area (say a town centre) is compared to a nearby rural area (or countryside) and the difference is used to quantify the impact of urbanization (e.g. Karl *et al*., 1988). However, the former approach is difficult to realize in practice. Thus, modelling is a convenient approach to study the impact of urbanization (e.g. Molders and Olson, 2004; Lamptey *et al*., 2005b) if the representation of urban land cover in the model is realistic. This is because a model simulation can first be performed without urban land cover over the region of interest, and the simulation repeated with urban land cover over the same region. Although, models are an abstraction of reality, the difference in these two model climates is an estimate of the effect of urbanization. The hypothesis is that the impact of urban land cover on the global weather and climate

*Correspondence to: Benjamin Lamptey, National Center for Atmospheric Research, Research Applications Laboratory, PO Box 3000 Boulder, CO 80307-3000, USA. E-mail: lamptey@ucar.edu
† Current address: International Water Management Institute, PMB CT 112, Cantonments, Accra, Ghana.

is negligible compared to that due to other types of land cover. However, urbanization may affect the weather and climate on spatial scales comparable to the urban scale, say perhaps, from tens to a few hundred kilometers or so. This is particularly so with respect to surface energy fluxes.

The urban impact on weather and climate processes at the regional scale, and smaller, can be of first-order significance (e.g. Shepherd and Jin, 2004). Buildings and urban land-use significantly impact the micro- and mesoscale flow fields, altering the wind, temperature, turbulence and radiation budget fields (e.g. Bornstein, 1987). It is necessary to have urban canopy parameterizations in mesoscale numerical models to approximate the drag, heating, radiation attenuation and enhanced turbulent kinetic energy produced by the sub-grid-scale urban elements. These urban parameterizations are necessary because mesoscale models do not have the spatial resolution to directly simulate the fluid dynamics and thermodynamics in and around urban structures. For example, in order to improve the representation of urban land cover in mesoscale meteorological models, Brown (2001) developed an urban canopy parameterization by adding drag to the momentum equation, mechanical turbulence production to the turbulent kinetic energy and turbulent length scale equations, anthropogenic and roof heat to the temperature equation, attenuation and trapping due to buildings to the short- and longwave radiation equations, and urban land-use properties to the SEB. An example of recent work on urban canopy models is the urban canopy parameterization work in the Weather Research and Forecasting (WRF) model (e.g. Jiang *et al*., 2008; Lin *et al*., 2008; Miao *et al*., 2008).

The difference between the relative warmth of a city UHI and its pre-urban conditions are due to changes in the SEB arising from

- anthropogenic heat through the tops and sides of buildings
- greater absorption of incoming shortwave radiation as a result of urban canyon geometry
- decreased outgoing longwave radiation due to sky-view factor reduction by urban canyon geometry
- greater daytime storage (and nocturnal release) of solar energy due to thermal properties of urban building materials
- outgoing longwave radiation decreased by elevated pollutant layers, and
- increased convective heat due to reduced latent heat flux from non-porous surfaces

The anthropogenic component of the magnitude of the surface heat-island at a particular location (and time) needs to take into consideration possible topographic influences such as elevation differences and bodies of water such as rivers, bays and lakes. Other factors include meteorological conditions such as cloud cover and wind speed (e.g. Bornstein, 1987). Also, the expansion of urban land alters the surface energy balance, with a consequent increase in sensible heat flux at the expense of latent heat flux. Such repartitioning of surface energy fluxes is usually described by the Bowen ratio.

Using the surface energy balance, this work shows that urban land cover has a comparatively small impact on the global climate. Thus, incorporating realistic urban land cover in global climate models may not be critical at this time for certain climate prediction problems. However, incorporating realistic urban land cover in mesoscale atmospheric models is shown to be important depending on the domain where the model is run. This work utilizes a simple method to show that for certain geographical areas urbanization may critically influence the regional climate. The method used is a purely analytical approach that enables the impact of urbanization on the weather and climate over a given region and time to be assessed.

Snapshots (i.e. timeslices) of Chester County and surroundings near Philadelphia, Pennsylvania, in the USA, have been used to illustrate the importance or otherwise of urbanization at the regional scale. The choice of Chester County is based purely on the fact that data is available from earlier work done there (e.g. Arthur *et al*., 2000; Carlson and Arthur, 2000; Hebble *et al*., 2001). The results presented must be considered preliminary as the method needs to be tested over other geographical regions.

The objective of this work is to assess the effect of urbanization in comparison with other land cover types on (1) global climate, and (2) regional climate using the SEB with empirical values and remotely sensed data. The idea is to illustrate the influence of urban landscapes on the global and regional climates.

A description of the data used in this work is given in the next section. This is followed by the results, discussion and finally conclusion in the subsequent sections.

2. Data

2.1. Global data

The global land-use data (Tables 1 and 2) used for the estimates of the area covered by each land-use type, were obtained from the World Resources Institute (WRI) website (http://earthtrends.wri.org/datatables/index.php?theme=9, 2003). The data is from the Land Area Classification by Ecosystem Type data table. For the purpose of this work, the Earth was represented by only five land-use categories as follows: water, forest, urban, short (agricultural) vegetation and desert. Thus, the different phases of water (i.e. snow and ice covered regions) in the land-use data table were combined together and classified as water. The fraction of the Earth covered by each land cover type (Table 3) was computed using the values in Tables 1 and 2. Note that the fraction for water does not include the ocean as the database used is for land areas. The values of Bowen ratio for the different land-use categories (Table 4) were mainly taken from Glickman (2000). It assumes a constant Bowen ratio throughout the year. Three values of the annual surface total

DOI: 10.1002/joc

Table I. Total land area (in square kilometers) classified as.

	Forest				Mixed					
	Evergreen		Deciduous			Shrublands		Savannas		Grasslands
	Needleleaf	Broadleaf	Needleleaf	Broadleaf		Closed	Open	Woody	Non-woody	
World	4,858,707	13,479,749	1,959,892	2,229,308	9,930,103	2,636,901	20,706,263	8,405,816	7,607,497	10,541,721

source:http://earthtrends.wri.org/datatables/index.php?theme=9

Table II. Remaining total area (in square kilometers) classified as.

	Permanent wetlands	Croplands	Urban and built-up	Cropland/Natural vegetation mosaic	Snow and ice	Barren or sparsely vegetated	Water bodies
World	984,328	15,206,323	256,332	11,586,898	2,621,872	18,332,436	3,494,824

source:http://earthtrends.wri.org/datatables/index.php?theme=9

Table III. Percentage of land-use categories on the Earth.

Type	Fraction
Desert	12.3
Forest	31.3
Urban	0.2
Vegetation	52.1
Water	4.1

Table IV. Bowen ratio of land-use categories on the Earth.

Type	Bowen ratio	Source
Desert	5.0	Glickman, 2000
Forest	0.5	Glickman, 2000
Urban	1.5	Brown, 2001
Vegetation	0.5	Glickman, 2000
Irrigated orchards or grass	0.2	Glickman, 2000
Water	0.1	Glickman, 2000

net radiation were used. The first value was estimated from simple radiative transfer theory using the planetary albedo. The second was again computed from simple radiative transfer theory but using an estimated global land-only albedo. The third set was monthly global land surface total net radiation (Table 5). This monthly data was obtained from the National Aeronautics and Space Administration (NASA) Global Energy and Water Cycle Experiment Surface Radiation Budget (GEWEX SRB) project (http://gewex-srb.larc.nasa.gov/) (e.g. Mikovitz, 2007, personal communication). The land-only albedo used in the computation of the surface total net radiation (i.e. G_{emp2} in Table 6) was estimated from the Moderate Resolution Imaging Spectrometer (MODIS) data.

The MODIS is an instrument aboard the Earth Observing System (EOS) Terra (EOS AM) and Aqua (EOS PM) satellites. The timing of Terra's orbit around the Earth is such that, Terra passes from north to south across the equator in the morning. Aqua's timing is such that, it passes south to north over the equator in the afternoon. Terra MODIS and Aqua MODIS are viewing the entire Earth's surface every one to two days, acquiring data in thirty-six spectral bands, or groups of wavelengths (http://modis.gsfc.nasa.gov/about/). The MODIS data was used to obtain an estimate of global land area albedo (Figure 1). A description of the MODIS product can be obtained from (http://lpdaac.usgs.gov/modi/mcd43c3v4.asp; Gao *et al*., 2005; Schaaf *et al*., 2002).

2.2. Chester County, Pennsylvania, data

The area of Chester County is 183 732 hectares or 709 square miles [equivalent to approximately a square of 42.7 km (e.g. Carlson, 2007, personal communication)]. The values of fractional land-use coverage for urban, agricultural, forest and water in Chester County, Pennsylvania (Table 7), were obtained from Arthur *et al*., 2000. There was no data for desert land-use category for Chester County. During the nine-year period (i.e. 1987–1996), progressive increase in urban, or built-up land, occurred largely at the expense of farmland, whereas forested area decreased only slightly. Detailed information about Chester County can be obtained from (e.g. Arthur *et al*., 2000 and Carlson and Arthur, 2000).

Regional monthly values of surface radiation (shortwave, longwave and total net) were obtained from the NASA GEWEX SRB project (http://gewex-srb.larc.nasa.gov/). The radiation fluxes are for a $1^\circ \times 1^\circ$ grid box with centre coordinates of 39.5 °N and 75.5 °W. This surface radiation data for West Chester Pennsylvania is GEWEX SRB shortwave version 2.81, longwave version 2.5 (e.g. Mikovitz, 2007, personal communication). Table 8 shows the seasonal values of the Bowen ratio.

3. Method

3.1. Global scale

To assess the effect of urbanization on global climate, estimates of a reasonable average flux of sensible and

DOI: 10.1002/joc

Table V. 1987, 1988, 1991, 1993 and 1996 global land areas total net radiation (in Wm^{-2}) at the surface.

	Jan	Feb	Mar	Apr	May	Jun	Jul	Aug	Sep	Oct	Nov	Dec	Mean
1987	81.15	86.96	89.65	84.48	82.53	80.61	79.41	77.72	77.54	82.48	80.49	79.78	81.90
1988	82.22	87.52	83.80	83.77	80.44	80.80	83.79	81.24	80.04	77.28	77.62	79.61	81.68
1991	80.80	89.96	85.47	86.62	84.24	84.17	82.19	79.55	79.20	79.11	81.49	77.04	80.80
1993	79.86	83.29	85.28	85.48	84.58	83.19	84.66	82.89	81.33	80.38	81.95	80.42	82.77
1996	83.27	87.23	86.80	85.96	84.64	82.37	83.59	83.55	84.09	84.92	81.79	82.40	84.22

Table VI. Table of experiments.

Experiment	Scale	Period	Remarks	Net radiation data
G_1	global	annual	used constant β, $Q_G = 0$, $\alpha_p = 0.30$, simple SEB equation	empirical
G_2	global	annual	used constant β, $Q_G = 0$, $\alpha_l = 0.24$, simple SEB equation	empirical
G_{8796}	global	annual	used constant β, $Q_G = 0$, simple SEB equation	NASA
R_{8796}	regional	annual	used constant β, $Q_G = 30\%$ Q, simple SEB equation	NASA
R_{sea}	regional	seasonal	used constant β, detailed SEB equation	NASA
$R_{\beta sea}$	regional	seasonal	used seasonal β, detailed SEB equation	NASA

Where β is Bowen ratio, Q_G is ground heat flux, α_p is planetary albedo, α_l is global land area albedo, Q is total surface net radiation and SEB is Surface Energy Balance equation.

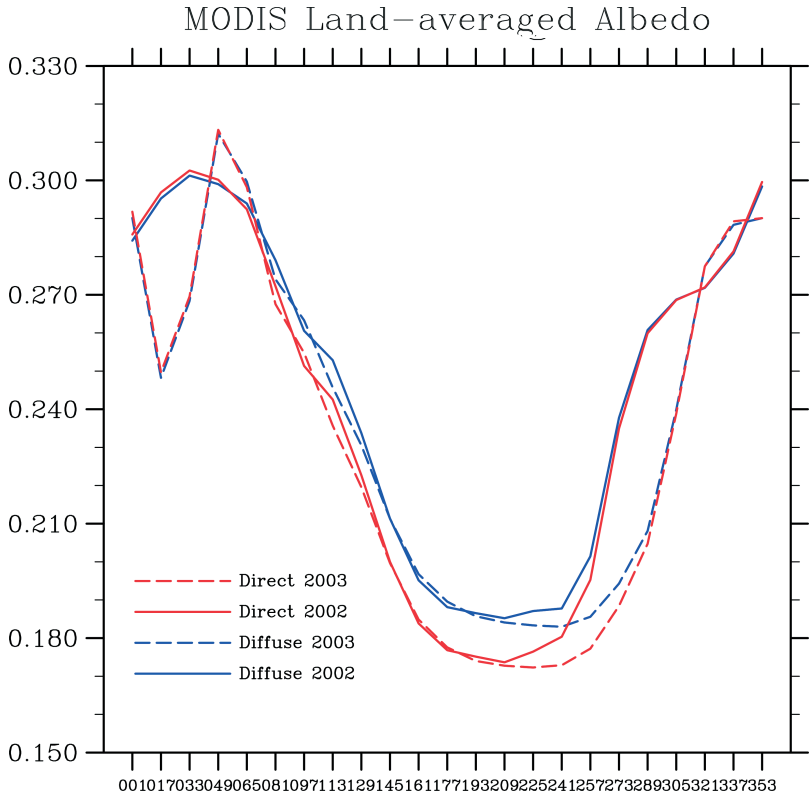

Figure 1. Area-averaged land albedo for 2002 and 2003 for direct and diffuse solar radiation. The x-axis is Julian day.

latent heat for each of five different types of land-use categories (water, forest, urban, short vegetation and desert) were computed. A fractional percentage for each land-use category was estimated over the globe. The sensible and latent heat fluxes due to each land cover type were computed based on the fractional coverage (i.e. proportionate heat fluxes). The magnitude of the urban effect was assessed with respect to computed estimates of sensible and latent heat fluxes. It was then assumed that the urban areas would otherwise be short vegetation if no cities or urban centres were to exist, and the fluxes for the vegetation land-use category were re-calculated with the urban areas replaced by vegetation. The assumption to replace urban land areas with vegetation was made

DOI: 10.1002/joc

Table VII. The percentage of land in each class for Chester County, Pennsylvania.

	Urban or built-up	Agricultural (bare/vegetated)	Forest	Water
1987	10.9	71.8	16.8	0.5
1988	11.6	70.8	16.9	0.6
1991	15.1	69.3	15.1	0.5
1993	16.3	67.5	14.7	0.4
1996	19.0	65.9	14.7	0.3

Source: Reproduced from Arthur *et al*., 2000 (http://www.informaworld.com)

Table VIII. Daytime Bowen ratio by land use and season. Average moisture conditions.

Land use	Spring	Summer	Autumn	Winter
Water (fresh and sea)	0.1	0.1	0.1	1.5
Deciduous forest	0.7	0.3	1.0	1.5
Coniferous	0.7	0.3	0.8	1.5
Swamp	0.1	0.1	0.1	1.5
Cultivated land	0.3	0.5	0.7	1.5
Grassland	0.4	0.8	1.0	1.5
Urban	1.0	2.0	2.0	1.5
Desert shrubland	3.0	4.0	6.0	6.0

source (Paumier and Brode, 2004)

because it is obvious that urban sites are springing up in previously vegetated areas.

The global computations were done in three different ways. First, surface total annual net radiation was estimated from radiative transfer theory (see Figure 2 and Appendix A) using an albedo of 0.30 (i.e. planetary albedo) in the computations. Second, the previous computation was repeated but using an estimated global land albedo of 0.24. This land-only albedo was estimated from Figure 1 by taking the average of 0.30 (maximum value) and 0.18 (minimum value) to obtain 0.24. This land-only albedo climatology was obtained from only two years of MODIS data (2002 and 2003) so the results should be considered as preliminary. The computation of the global annual sensible and latent heat fluxes due to each land cover type was done using these estimated global values of total net radiation, ground heat flux and Bowen ratios for the different land-use categories. The Bowen ratio, β, is given by

$$\beta = \frac{Q_H}{Q_E} \tag{1}$$

where Q_H is sensible heat (turbulent) and Q_E is latent heat (turbulent). The calculation of the turbulent heat fluxes was done by simultaneously solving the surface energy balance and Bowen ratio equations. The energy balance for a simple plane surface may be written as

$$Q^* = Q_H + Q_E + Q_G \tag{2}$$

where Q^* is net radiation, and Q_G is (primarily) conductive heat flux into or out of the surface. Ideally, the energy balance equation should contain a term for the anthropogenic heat flux as well as advective heat flux (see next section). However, Equation 2 was used for the global scale computations with the anthropogenic heat flux, Q_F set to zero, since it is difficult to obtain estimates of Q_F at the global scale.

The methods mentioned above used empirical global annual estimates of the components of the surface energy balance equation. Thus, they do not refer to any particular year (experiments G_{emp1} and G_{emp2} in Table 6).

The third experiment used surface total net radiation data for five specific years. The computation of the global annual sensible and latent heat fluxes were calculated for 1987, 1988, 1991, 1993 and 1996. The yearly values were computed from monthly global land surface total net radiation values obtained from NASA. This third computation, experiment G_{8796} in Table 6, enables a direct comparison of the relative impact of the land cover types at the global scale with that at a regional scale (i.e.

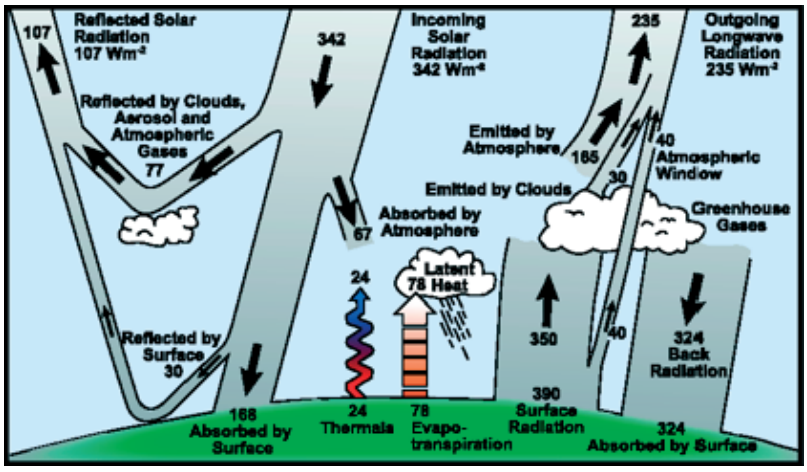

Figure 2. Estimate of Earth's annual and global mean energy balance. Source: (IPCC, 2007).

DOI: 10.1002/joc

Chester County) as there is data for the same period at the regional scale.

3.2. Regional scale

Energy fluxes in the UHI have implications of scale. For example, individual landscape units, like urban canyon, land-use zones or whole cities have completely different scale considerations. Equation 2 above is a simplification of the full equation. The equation should be

$$Q^* + Q_F = Q_H + Q_E + \Delta Q_S + \Delta Q_A \qquad (3)$$

Oke (1982)and Arnfield (2003) for total urban landscapes, where the energy fluxes are evaluated through the top of an imaginary volume at the upper margins of the Urban Canopy Layer (UCL). Q_F is anthropogenic energy releases within the volume; ΔQ_A is net advection through the sides of the volume; and ΔQ_S is storage heat flux and represents all energy storage mechanisms within the volume, in air, trees, building fabrics, soil, etc. In practice, by virtue of heat capacities for air and solid fabric, ΔQ_S can normally be equated to the aggregate Q_G for all air-solid interfaces within the volume (e.g. Arnfield, 2003). A central urban site surrounded by fairly uniform building density can be considered free of advection, so that ΔQ_A can be ignored. This assumption is, however, not reasonable for an area near the rural/urban boundary, or where land use is variable (e.g. Oke, 1987). Also, the advective heat flux is small if the site is horizontally extensive (e.g. Masson, 2006). Chester County and its surroundings were assumed to be extensive enough so as to be free of advective heat flux. Using the assumption of the urban site being free of advection, Equation 3 becomes

$$Q^* + Q_F = Q_H + Q_E + Q_G \qquad (4)$$

Equation 4 is the surface energy balance for the urban canopy and Equation 2 for the other land cover types at the regional scale (e.g. over Chester County).

The effect of urbanization on the climate of Chester County and its surroundings, Pennsylvania in the USA, was considered for 1987, 1988, 1991, 1993 and 1996. This is a period during which Chester County became more urbanized (e.g. Arthur *et al.*, 2000). The month of January was used to represent the winter season while July represented the summer. Values of the monthly total net radiation for these months were used in the calculation of the heat fluxes over Chester County.

Three sets of computations were done over Chester County. The first used the simple surface energy balance equation as used for the global scale (i.e. Equation 2) but with ground heat flux not equal to zero (experiment R_{8796} in Table 6). This is because the average annual ground heat flux for a region is not zero as is the case with the global equivalent. This experiment, R_{8796}, enables a comparison with the global scale calculations from experiment G_{8796}. The second set of computations used the relatively more detailed surface energy balance equation (i.e. Equation 4) but with a constant β for each land-use type throughout the year (i.e. experiment R_{sea} in Table 6). The third experiment was a repetition of the second but using seasonal values of β (i.e. experiment $R_{\beta sea}$ in Table 6). In the R_{sea} and $R_{\beta sea}$ experiments, seasonal values of the turbulent fluxes were computed using a constant Bowen ratio and seasonal values of Bowen ratio respectively. Table 8 shows the seasonal values of the Bowen ratio.

Thus, both annual and seasonal values of the turbulent fluxes were computed (experiments R_{8796}, R_{sea} and $R_{\beta sea}$ in Table 6). The monthly surface total net radiation values for January were used to represent the winter season, while the July values represented summer of each year. As stated earlier, these were obtained from the GEWEX SRB project. The annual values of the turbulent fluxes were obtained by solving the Bowen ratio (Equation 1) and the simple surface energy balance equation (i.e. Equation 2) simultaneously for all the five different land cover types for each of the five years. The heat fluxes were multiplied by the values of the fractional land cover for each type to obtain the proportionate heat fluxes. In computing these fluxes, a constant β (Table 4) for each land cover type was used.

For the seasonal values of the fluxes, the relatively more detailed surface energy balance equation was used. The surface energy balance equation for the urban canopy (i.e. Equation 3) and the Bowen ratio equation (i.e. Equation 1) were solved simultaneously to obtain the sensible and latent heat fluxes due to urban land cover over Chester County. For the other land cover types over Chester County (water, forest and agriculture), Equations 4 and 1 were solved simultaneously to obtain the turbulent fluxes.

Ideally, the ground heat flux (or heat entering the underlying soil), Q_G, should have been estimated from

$$Q_G(0) = \frac{\sqrt{2}k'\Delta T_0}{D} sin(\omega t + \pi/4) \qquad (5)$$

which is the solution to

$$Q_G(z) = -k'\frac{\delta T}{\delta z} \qquad (6)$$

where z is the depth into the soil (e.g. Liebethal and Foken, 2007), k' is thermal conductivity, and T is temperature of the soil. Since it is difficult to obtain the amplitude of the diurnal or annual temperature cycle, ΔT_0, over a large region like Chester County and surroundings, a different method was used to obtain the ground heat flux.

The ground heat flux was estimated as a percentage of the total net radiation. The magnitude of the flux into the ground, Q_G, is $\sim 10\%$ of the net radiation magnitude during daytime, increasing to $\sim 50\%$ at night (e.g. Wallace and Hobbs, 2005; Liebethal and Foken, 2007). An average value of the ground heat flux was obtained by using 30% (average of 10 and 50%) of the total net radiation. The ground heat fluxes were computed

DOI: 10.1002/joc

for both the annual and seasonal cases since the average annual and seasonal ground heat fluxes over a given region are not zero.

For the anthropogenic heat flux, a value of 60 Wm^{-2} was estimated for the winter season and 40 Wm^{-2} for the summer season. The estimates were based on the diurnal and seasonal anthropogenic heating profile for Philadelphia developed by Sailor and Lu (2004). In arriving at the diurnal and seasonal anthropogenic heating profiles for urban areas, Sailor and Lu (2004) used heat released from the building sector, transportation sector and metabolism. Each component was developed separately based on a population density formulation. The heat sources used included heat from vehicular traffic, heat from electricity consumption, heat from heating fuels and heat released from human metabolism.

The surface energy balance equations (for the urban canopy, Equation 4, and the other land cover types, Equation 2, respectively) and the equation for the Bowen ratio were solved simultaneously to obtain the monthly values of sensible and latent heat fluxes over Chester County.

4. Results

4.1. Global scale results

4.1.1. Using empirical values

The results in this section are based on empirical values and thus, do not refer to any specific year. The annual surface total net radiation is obtained from radiative transfer theory.

As the surface heat budget must balance, the radiative fluxes constrain the sum of the sensible and latent heat fluxes in the annual global mean energy budget (e.g. Kiehl and Trenberth, 1997). This implies, at the surface, the annual global average of the ground heat flux, Q_G is approximately 0 Wm^{-2}

The global average solar irradiance is equal to 340 Wm^{-2}. We assume approximately 50% (i.e. 30% is reflected, and another 20% is absorbed in the atmosphere) of this shortwave radiation is either reflected or absorbed by gases/clouds (e.g. Lenoble, 2001). This implies mean surface solar irradiance of approximately 170 Wm^{-2}

Assuming a surface temperature of T_S equals 15 °C, gives $\sigma T_S^4 \approx 390$ Wm^{-2} as the upward infrared (IR) irradiance and a downward IR irradiance at the surface is $\approx 0.85\ \sigma T_S^4 \approx 330$ Wm^{-2}. Thus, net thermal IR irradiance is approximately equal to 60 Wm^{-2} and the net total surface radiation (i.e. 170 −60) is $Q^* = 110$ Wm^{-2}. See Appendix A for the derivation. Assume Q^* is 100 Wm^{-2}

From the conservation of water mass the latent heat flux is equal to the global mean rate of precipitation (e.g. Kiehl and Trenberth, 1997). This implies the annual mean evaporation rate is approximately equal to the annual mean precipitation rate. This is approximately 1 m/year. The latent heat flux is the energy required to evaporate 1 m/year. This energy is 2.5×10^6 J/kg $\times$ 10^3 kgm^{-3} where 2.5×10^6 J/kg is the latent heat of vaporization and 10^3 kgm^{-3} is the density of water. Thus,

$$Q_E = \frac{2.5e9}{\pi e7} \tag{7}$$

where the denominator is the number of seconds in a year. Q_E is thus 80 Wm^{-2}. Thus, on average, 80% of the energy available for radiation (globally) is used for evaporation. The remainder must be sensible heat and is $Q_H = 20$ Wm^{-2}

Local partitioning between Q_H and Q_E depends on water availability. Using the values of Bowen ratio for the five different types of land-use categories in Table 4, and the fact that the sum of the sensible and latent heats equals the total net radiation at the surface, the values in Table 9 were obtained for each land-use category.

The proportionate sensible heat (and latent heat) due to each land cover type, is the product of the fraction of land cover type and the calculated sensible (and latent heat) associated with that land cover type. Table 10 shows the proportionate global sensible and latent heat fluxes for the five land-use categories. The fraction of land that is urban is 0.2% (see Table 3). Using the values in Table 9, the proportionate sensible and latent heat fluxes for the urban land cover were

$$0.002 \times 60 = 0.12 \tag{8}$$

$$0.002 \times 40 = 0.08 \tag{9}$$

respectively (Table 10). Urbanization produces 0.12 Wm^{-2} (sensible heat) and 0.08 Wm^{-2} (latent heat)

Table IX. Global annual sensible and latent heat fluxes (Wm^{-2}) using planetary albedo (0.30) and land-only albedo (0.24).

Type	using $\alpha = 0.30$		using $\alpha = 0.24$	
	Sensible	Latent	Sensible	Latent
Water	9.1	90.9	8.4	83.6
Forest	33.3	66.7	30.6	61.3
Urban	60.0	40.0	55.2	36.8
Vegetation	33.3	66.7	30.7	61.3
Desert	83.3	16.7	76.6	15.3

Table X. Proportionate global annual sensible and latent heat fluxes (Wm^{-2}) using planetary albedo (0.30) and land-only albedo (0.24).

Type	using $\alpha = 0.30$		using $\alpha = 0.24$	
	Sensible	Latent	Sensible	Latent
Water	0.4	3.7	0.3	3.4
Forest	10.4	20.9	9.6	19.2
Urban	0.1	0.1	0.1	0.1
Vegetation	17.4	34.7	16.0	31.9
Desert	10.3	2.0	9.4	1.9

DOI: 10.1002/joc

annually. The results (i.e. Table 10) shows that on a global scale the effect of urbanization on climate is the least of all the five land-use categories.

The fraction of land that is vegetation is 52.1%. If the urban areas were to be vegetation, the sensible heat flux due to vegetation, 17.4 Wm^{-2} remains virtually the same while the latent heat value changes from 34.7 Wm^{-2} to 34.9 Wm^{-2}.

The above results were obtained by solving the surface energy balance equation and the Bowen ratio equations. The value of the surface total net radiation in the above computations was obtained using the global planetary albedo. The surface total net radiation was re-calculated using an estimated global land-only albedo (i.e. 0.24), and the corresponding turbulent fluxes from this calculation (experiment G_2 in Table 6) are shown in Tables 9 and 10 as well. The values are close to that obtained using the planetary albedo.

4.1.2. Using NASA data

The turbulent fluxes were computed again using NASA data for the global land area surface total net radiation for 1987, 1988, 1991, 1993 and 1996. Although urban land cover did not produce the least turbulent fluxes (Figure 3), it did produce the least proportionate turbulent fluxes (Figure 4). The computations were done using a constant value of β as in the empirical calculations above. The fact that urban land cover gives the least proportionate turbulent fluxes is the same result obtained using the empirical annual surface total net radiation in the previous section.

4.2. Regional scale results

At the regional scale, both annual and seasonal values of the turbulent fluxes were computed (experiments R_{8796}, R_{sea} and $R_{\beta sea}$ in Table 6). The anthropogenic heat flux was estimated from the seasonal anthropogenic heating profile for Philadelphia (Sailor and Lu, 2004). The summer value used in this work was 60 Wm^{-2} and the winter value was 40 Wm^{-2} (Table 11).

In computing the annual and proportionate annual fluxes, a constant β (Table 4) for each land cover type was used. Urban land cover type produced the largest sensible heat flux but the smallest latent heat flux in all the five given years (Figure 5). However, vegetation produced the largest proportionate sensible and latent heat fluxes (Figure 6). This is obviously due to vegetation having the largest fractional coverage.

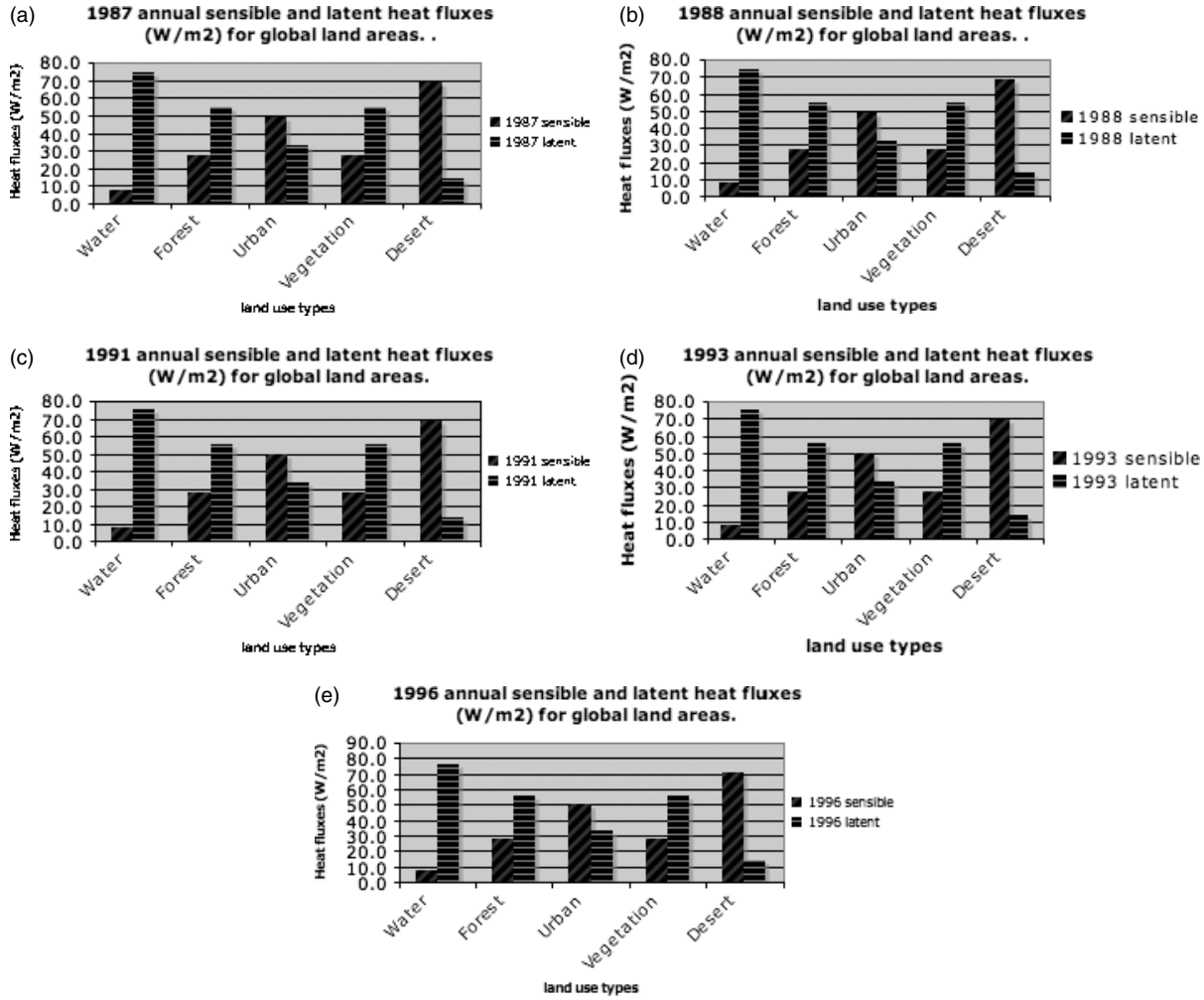

Figure 3. 1987, 1988, 1991, 1993 and 1996 annual sensible and latent heat fluxes for global land area (W/m2).

DOI: 10.1002/joc

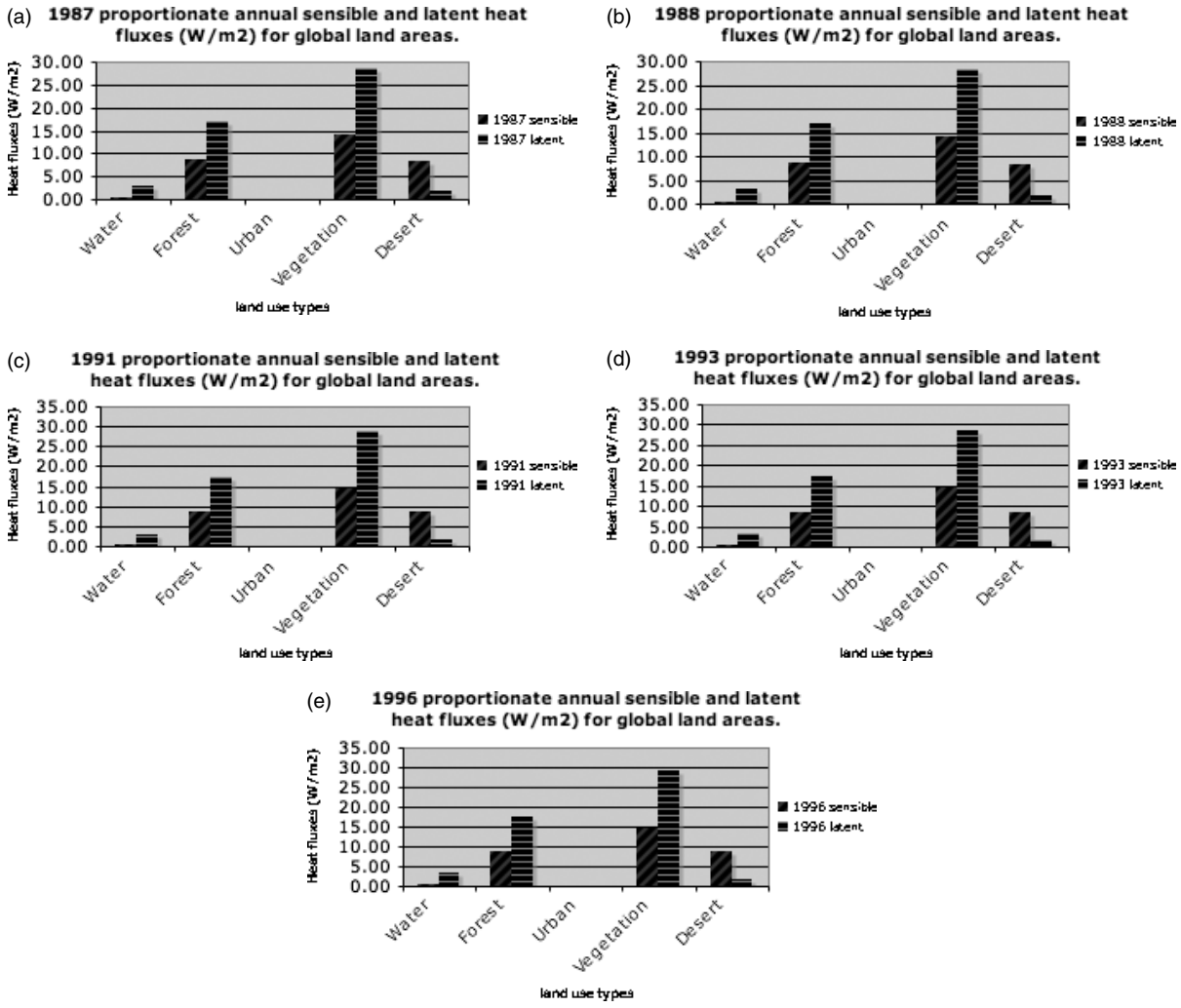

Figure 4. 1987, 1988, 1991, 1993 and 1996 proportionate annual sensible and latent heat fluxes for global land area (W/m2).

Table XI. 1987, 1988, 1991, 1993 and 1996 total net radiation, ground and anthropogenic heat fluxes (in Wm^{-2}) for Chester County, PA.

Type	1987		1988		1991		1993		1996	
	Winter	Summer	Winter	Summer	Winter	Summer	Winter	Summer	Winter	Summer
Total net radiation	21.7	157.9	25.7	144.8	27.3	127.5	19.8		13.4	149.8
Ground heat flux	−6.5	−47.4	−7.7	−43.4	−8.2	−38.3	−5.9	−40.3	−4.0	−44.9
Anthropogenic heat flux	60.0	40.0	60	40	60	40	60	40	60.0	40.0

Recall that the seasonal values of the turbulent fluxes were computed using (1) a constant value of β for each land cover type, and (2) seasonal values of β for each land cover type. The computation using the constant value of β (Table 4) indicates urban land cover produces the largest sensible heat flux (but least latent heat flux) in all the five given years. A striking observation is that the urban effect is magnified during summer (Figure 7) as the values of summer sensible heat fluxes are an order of magnitude larger than their corresponding winter values for all the five given years. The magnified urban effect during summer is in agreement with the modelling results of (e.g. Lamptey *et al*., 2005b) and (e.g. Trusilova *et al*., 2008). Vegetation produced the largest sensible and latent fluxes during both seasons in all the five years (Figure 8). This is obviously due to the large fractional coverage of vegetation.

The seasonal dependence of the Bowen ratio was investigated by using the seasonal values of β for each land cover type (Table 4) to re-compute the turbulent and proportionate turbulent fluxes. This is experiment $R_{\beta sea}$ in Table 6. The results indicated that urban land cover produced the largest sensible and latent heat fluxes during both seasons (Figure 9) in all the years. Here,

DOI: 10.1002/joc

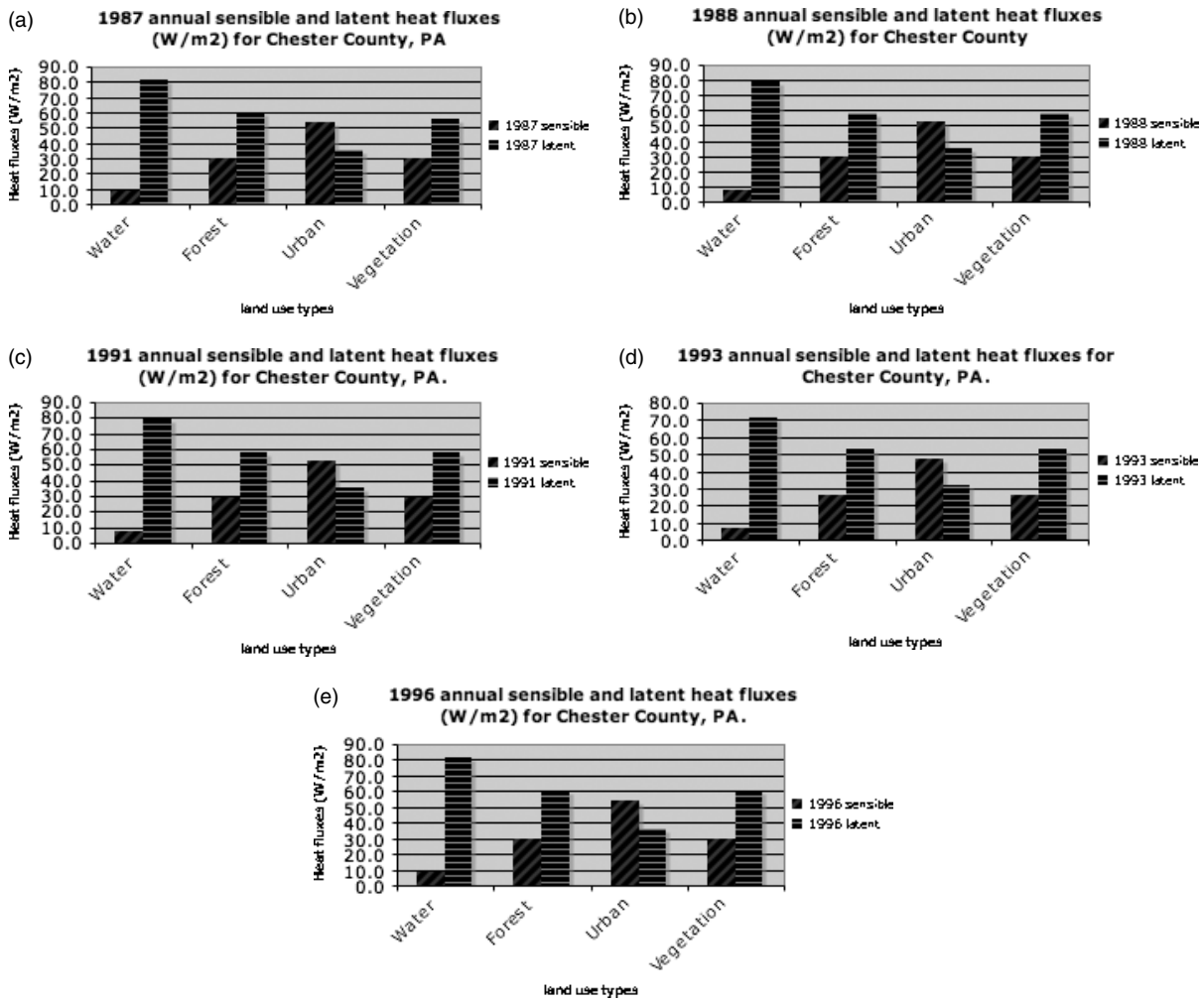

Figure 5. 1987, 1988, 1991, 1993 and 1996 annual sensible and latent heat fluxes (W/m2) for Chester County, PA.

even though the urban effect is magnified during the summer, the winter and summer values have the same order of magnitude with regards to the sensible heat fluxes. For example, the winter sensible heat flux for 1987 was 126.5 Wm^{-2} while the corresponding summer value was 427.4 Wm^{-2}. Except for 1996, vegetation produced the largest proportionate turbulent fluxes (Figure 10). The results indicate that the seasonal variation of β has a greater impact on the sensible heat flux. This is because the latent heat flux is limited by soil moisture.

4.3. Global versus regional results

Figures 4 and 6 are the proportionate annual turbulent fluxes for the five selected years at the global and regional scales, respectively. Constant Bowen ratios for each land cover type were used in computing the values in both figures. That is, the simple surface energy balance equation was used at the two different scales. It is evident that urban land cover does not give the least proportionate flux at the regional scale (Figure 6) like it does at the global scale (Figure 4). This is because the fraction of urban land cover at the regional scale is not the least. This is confirmed by the fact that the proportionate turbulent fluxes due to urban increases in magnitude from 1987 to 1996 as the fraction of land cover that is urban also increases (Table 7).

5. Discussion

5.1. Global scale

The estimates of the different components of the SEB obtained in this study are comparable to the values in Kiehl and Trenberth (1997) and references therein. Kiehl and Trenberth (1997) used a simple but appropriately tuned and observationally constrained radiation model. The references to other studies in Kiehl and Trenberth (1997) included both modelling and observational studies. Kiehl and Trenberth (1997) obtained a net shortwave flux of 168 Wm^{-2}, a net longwave flux of 66 Wm^{-2}, a latent heat flux of 78 Wm^{-2} and a sensible heat flux of 24 Wm^{-2}. These values are comparable to those obtained in this study: a net shortwave flux of 170 Wm^{-2}, a net longwave flux of 60 Wm^{-2}, a latent heat flux of 79 Wm^{-2} and a sensible heat flux of 33 Wm^{-2}.

One could argue that the different land-use categories have different albedos which should be taken into account when computing the net radiation. However, the planetary

DOI: 10.1002/joc

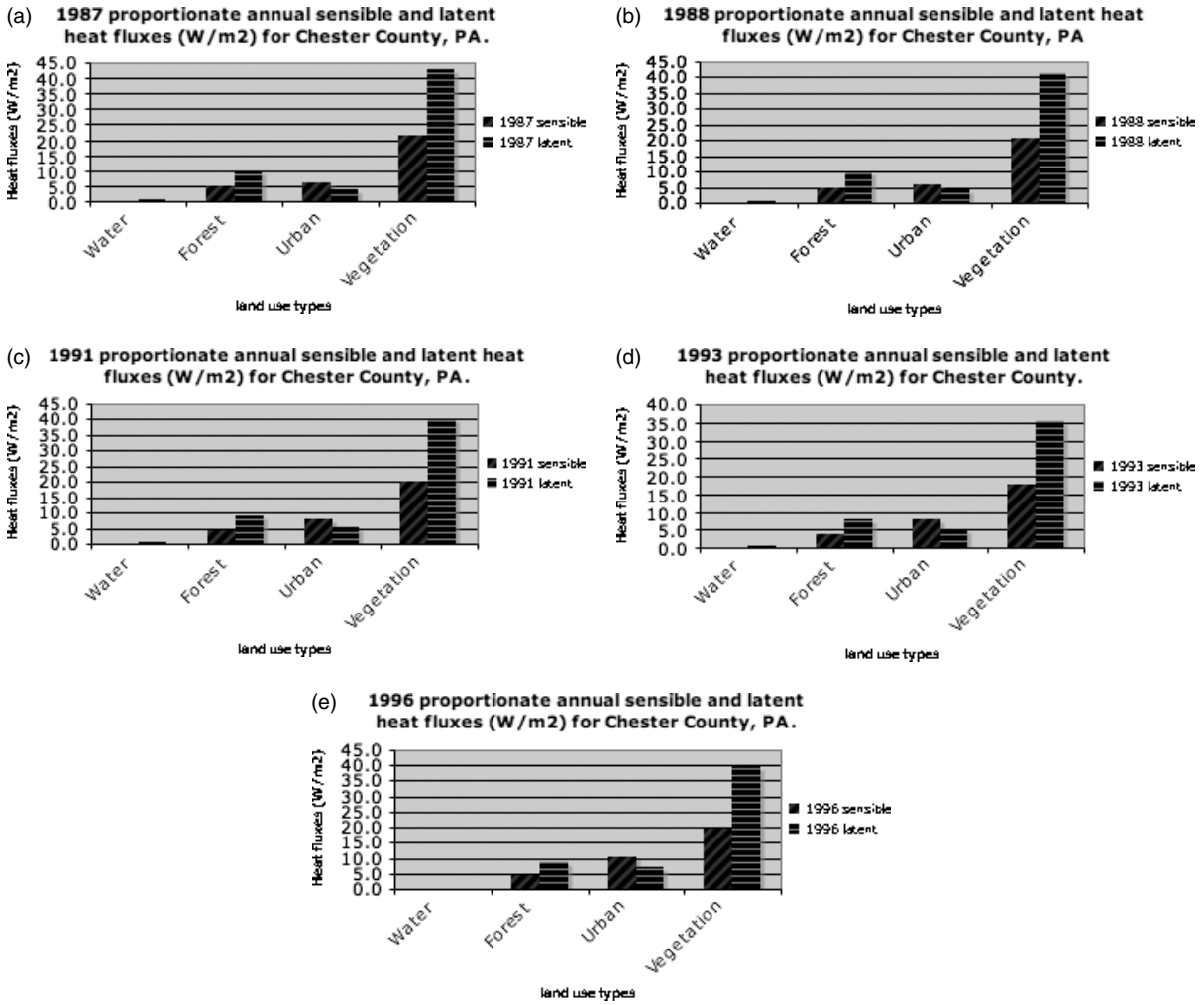

Figure 6. 1987, 1988, 1991, 1993 and 1996 proportionate annual sensible and latent heat fluxes (W/m2) for Chester County, PA.

albedo used in the calculation of the total net radiation (i.e. 30%) is the observed planetary albedo (e.g. Kiehl and Trenberth, 1997). This implies that the albedos of the different land-use categories have been taken into account. The caveat is that the planetary albedo includes the oceans, but the calculations in this study have been done for global land areas only. To investigate the impact of using the planetary albedo as against a global land-only albedo, the global annual turbulent fluxes were re-calculated using an estimated land albedo of 0.24. The results obtained were very close to the values obtained using 0.30. Thus, the general inferences or conclusions from this work will not change.

A point could also be made that the calculations at the global scale did not include other contributions of the urban landscape or human activities such as combustion, urban physiography, aerosol emissions, impact of irrigation, etc. Most of the aforementioned factors are hypothesized to have regional impacts. Assessing the overall impact of the different regional effects on the global climate is worth investigating. For instance, a two-way nesting between a global climate model and a regional climate model that has realistic representation of the different regional effects could be used for such a study. Second, the effects of aerosols for example, will be difficult to include in the global calculations because aerosol optical properties vary greatly due to chemical composition (e.g. Kiehl and Trenberth, 1997). However, since the purpose of this study is to illustrate the relative contributions of the different land-use categories on the turbulent heat fluxes, the method used is reasonable. The experiment could be repeated by including estimates of global anthropogenic heat flux when such an estimate becomes available. The approach used in this calculation is simple and flexible enough to accommodate more detailed information.

The importance of representing land cover types more realistically in grid cells of global climate models is evident by comparing Tables 9 and 10. For example, both forest and vegetation give the same sensible and latent heat fluxes but completely different proportionate sensible and latent heat fluxes. Also, using the values of the heat fluxes, deserts gave the largest sensible heat flux and water gave the largest latent heat flux (83.3 Wm^{-2} and 90.9 Wm^{-2} respectively in Table 9). But the largest proportionate sensible (17.4 Wm^{-2}) and latent heat (34.7 Wm^{-2}) fluxes came from vegetation (Table 10).

DOI: 10.1002/joc

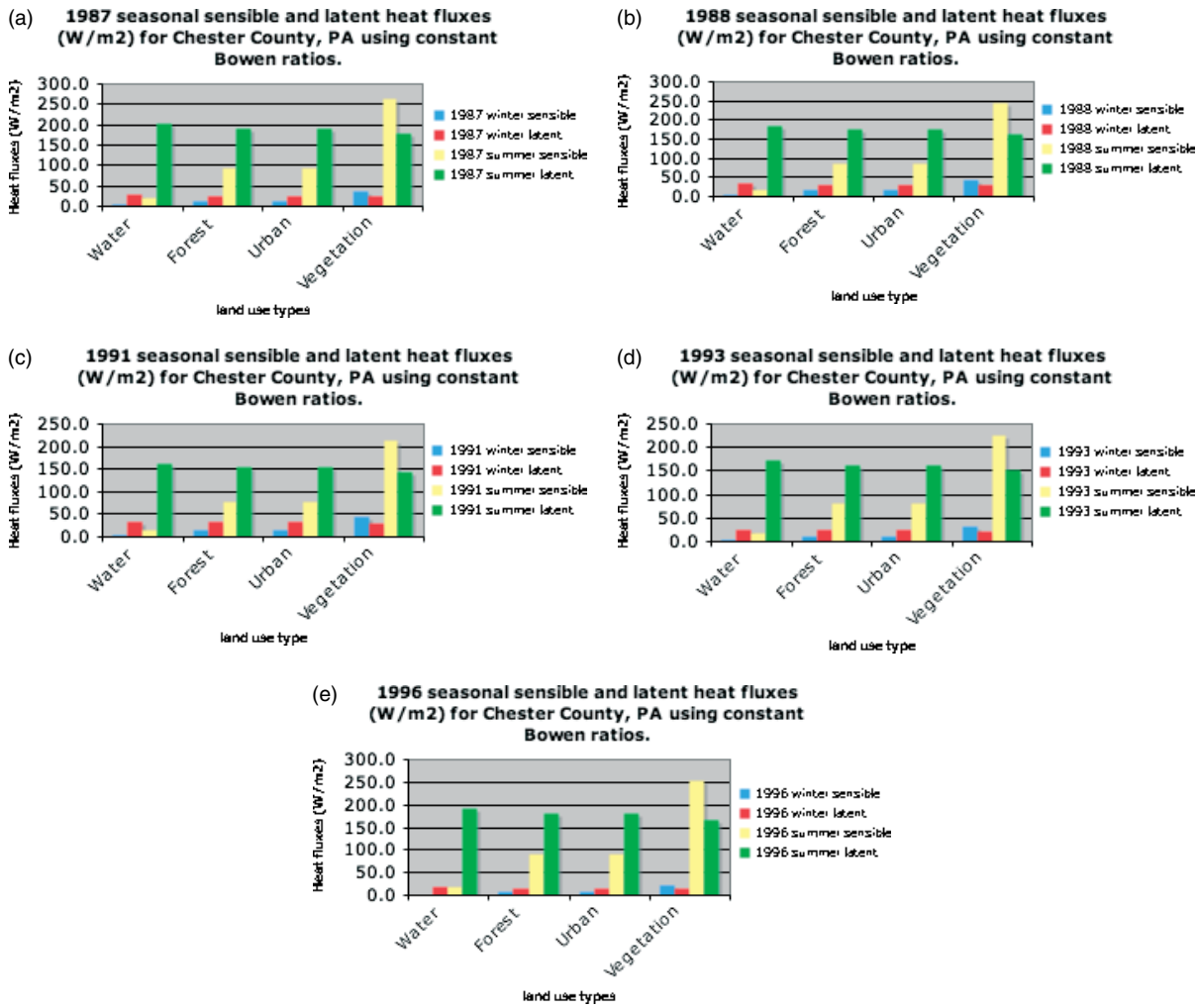

Figure 7. 1987, 1988, 1991, 1993 and 1996 seasonal sensible and latent heat fluxes (W/m2) for Chester County, PA, using constant Bowen ratios.

The effect of urbanization at the global scale is so minimal that, replacing the urban areas with vegetation did not change the proportionate sensible and latent heat fluxes due to vegetation. This is because of the relatively small fraction of the Earth covered by urbanization. An interesting point to consider is how important the urban effect will become globally, with the expected increase in urban area and population density. The increase in area of urban land cover could make the ground heat flux term in the energy balance equation relatively more important than it is at the moment. The increase in population density could also make the anthropogenic term relatively more important as energy usage will increase. Note that, at the regional scale, anthropogenic heat can exceed the net radiation for some cities. An example is the case of Manhattan, New York City, in 1967 (e.g. Oke, 1987). The heat released from Manhattan (40^0N), New York City in 1967, was for Q_F, 117 (annual value), 40 (summer value) and 198 (winter value) Wm^{-2}, and 93 Wm^{-2} for Q^*, the total net radiation. In some cities, Q_F is quite a significant source, and can surpass the net radiation especially during winter, as in the case of Manhattan above. The average anthropogenic heat flux (Q_F) depends on the average energy use by individuals and the city's population density (e.g. Oke, 1987). An important issue to consider is the fact that, with the current increasing spatial resolution of GCM and the expected growth in urban areas, there could be a critical threshold of influence of urbanization on the global climate based on this convergence (e.g. Jin *et al*., 2008).

The method used is a quick and simple way to estimate the urban effect at the global scale. However, the global method that uses empirical values of the surface total net radiation, lacks the ability to compute seasonal fluxes. This is a weakness in the approach as Bowen ratio and urban effect are season dependent. This seasonal dependence is particularly important at the regional scale but may become important at the global scale once a certain threshold of the fraction of urban land cover is reached. However, the method can be used to compute seasonal fluxes if seasonal estimates of the global ground heat flux are available. The approach that uses the remotely sensed data from NASA can be used to compute both annual and seasonal values for any given year. Although the results in this study suggest that the influence of a land cover type varies

DOI: 10.1002/joc

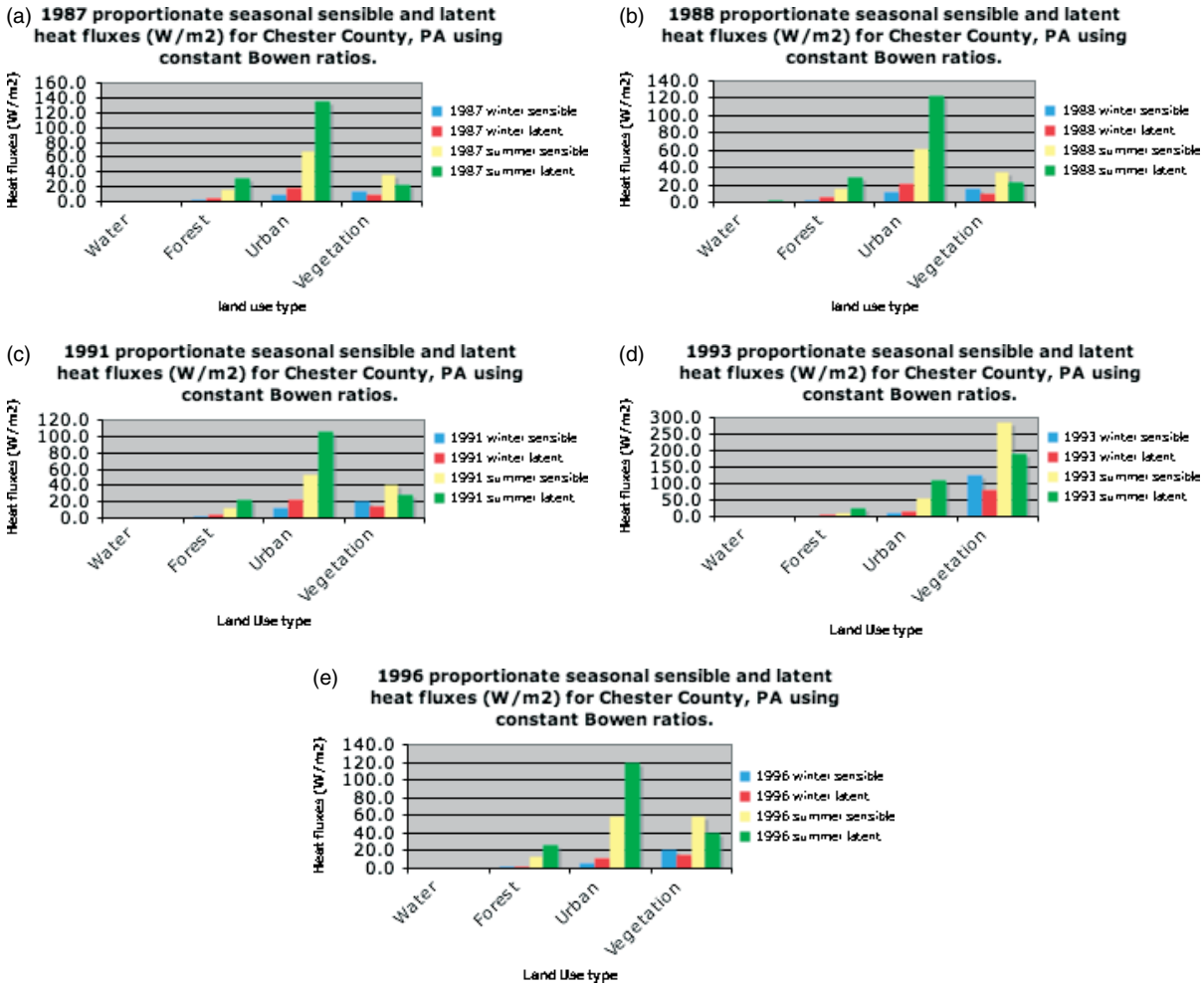

Figure 8. 1987, 1988, 1991, 1993 and 1996 proportionate seasonal sensible and latent heat fluxes (W/m2) for Chester County using constant Bowen ratios.

linearly (and monotonically) with the percent land cover area, a threshold behaviour to the response of urban land cover is hypothesized at the global scale. This hypothesis is because increasing anthropogenic heat flux may invalidate the linear scaling with larger cities. The anthropogenic heat flux may increase non-linearly with the size of the city.

Sensitivity studies could be performed to ascertain the threshold at which the urban effect would become important at the global scale. Also, it will be interesting to include the ocean waters in the calculation to see how that influences the calculations, especially at the global scale. This can be done if a database that has all the fractions of land cover is used.

An ideal or more detailed approach will be to repeat the computations for individual regions/surface types. This is because uncertainties do vary with surface type. Typically, the shortwave radiation uncertainty increases dramatically with bright surfaces because cloud detection is harder (i.e. bright deserts and/or snow/ice surfaces). Longwave radiation uncertainties increase with temperature inversions, particularly over ice and snow. Also, temperature discontinuities between the hot desert surface and the atmosphere lead to increased uncertainty (e.g. Stackhouse, 2007, personal communication). The objective of this study is only to assess the relative impacts of different land cover types on the turbulent fluxes. Since the actual or absolute values of the fluxes are not the focus of this study the issue of uncertainty can be overlooked for purpose of this study.

5.2. Regional scale

The analyses done here is at the county scale. The results would be very different if the analyses were at a finer scale. For example, the anthropogenic heat flux density at the urban core will be much higher than that at the county scale. Moreover, there are areas within the county that are heavily urbanized (e.g. Uwchlan Township, Hebble *et al.*, 2001, and Carlson, 2007, personal communication). The fact that the same value of anthropogenic heat flux (60 for winter and 40 for summer) was used for all the 5 different years is an important caveat. This is because the average anthropogenic heat flux (Q_F) depends on the average energy use by individuals and the city's population density (e.g. Oke, 1987; Sailor and Lu, 2004). Since the urban land cover over Chester County increased from 11% in 1987 to 19% in 1996, presumably the energy usage and population density in 1996 must be more than

DOI: 10.1002/joc

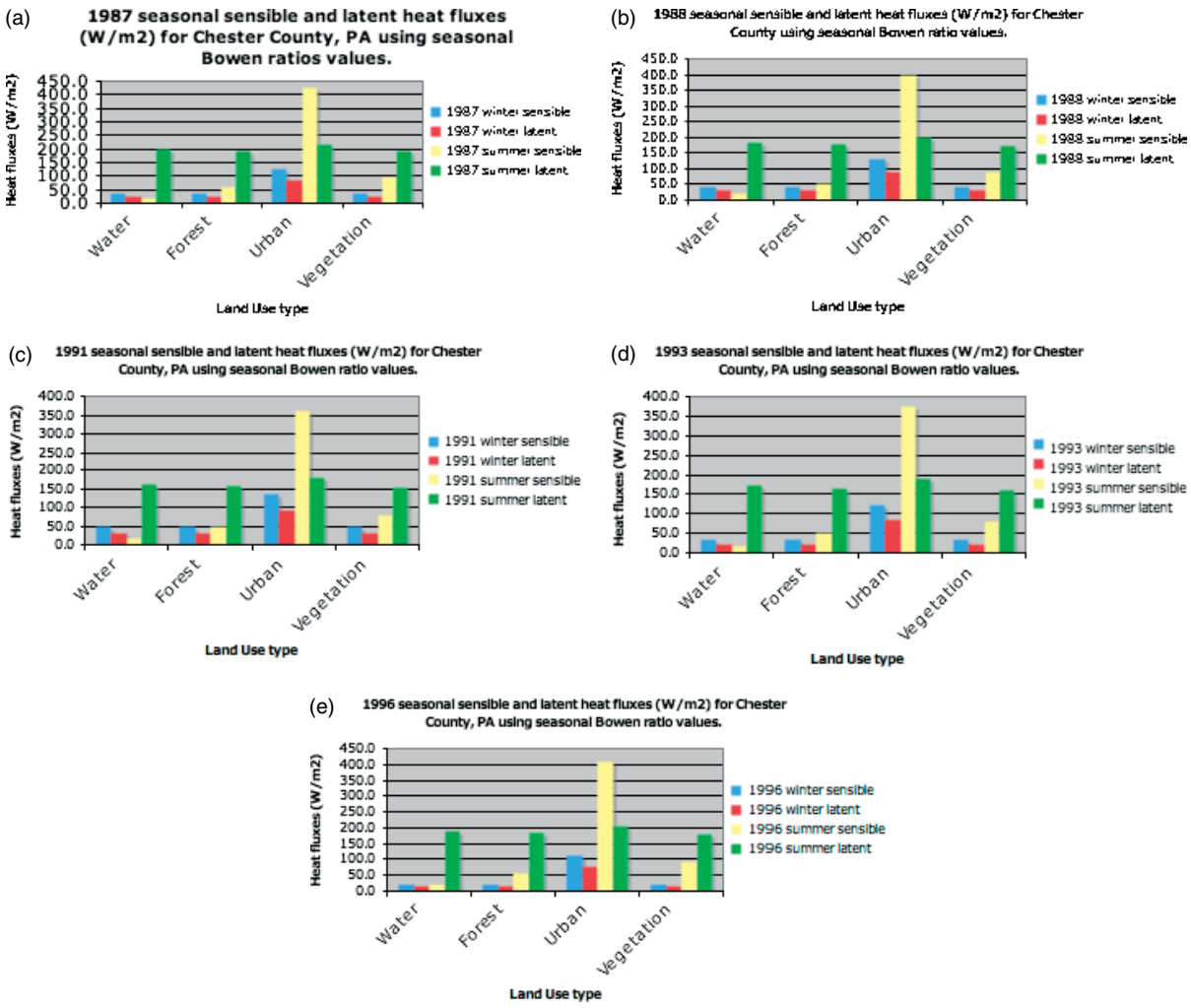

Figure 9. 1987, 1988, 1991, 1993 and 1996 seasonable sensible and latent heat fluxes (W/m2) for Chester County, PA, using seasonal Bowen ratios.

that in 1987. However, Sailor and Lu (2004) used data for the year 2000. A more robust method would be to find a way of scaling the anthropogenic heat in order to obtain a value for each year. Possibly, the gross domestic product (GDP) or the population density for each year could be used to do the scaling. This needs further investigation. Realistically, the estimates of the anthropogenic heat used in this study may be reasonable for 1996 but too high for 1987. However, since the point of this study is to illustrate the methodology used as well as the impact of the urban landscape, it is reasonable to use the values specified. The absolute values for 1987 could have been lower if actual estimates of anthropogenic heat flux for 1987 were used.

The availability of the total net radiation data simplified the computations at the regional scale as there was no need to have values of albedo, emissivity, thermal conductivity, etc., for different surfaces, which would have otherwise been needed to compute the various components of radiation (i.e. incoming and outgoing shortwave and longwave radiation). It must be noted that the total net radiation data is at a resolution of $1^\circ \times 1^\circ$, while the area of Chester County is about $1/2^\circ \times 1/2^\circ$. However, the coordinates of the grid box was centred more or less on Philadelphia. This makes the use of the data reasonable.

It has been assumed in this study that the whole of Chester County is extensive enough and land-use is not variable within the urban areas. Thus, it is reasonable to ignore the advective heat flux ΔQ_A (e.g. Masson, 2006) and (e.g. Oke, 1987).

The effect of interactions between the different land-use categories was not taken into account in this study at both the global and regional scales. It is speculated that the effect of the interactions will not change the results obtained. The absolute values of the heat fluxes may change but the relative contributions will not change. Some interactions (e.g. urban/vegetation) may be more important than other types of interactions. This needs to be investigated.

6. Summary and Conclusion

A simple analytical method has been used to show the relative importance of the contributions due to different

DOI: 10.1002/joc

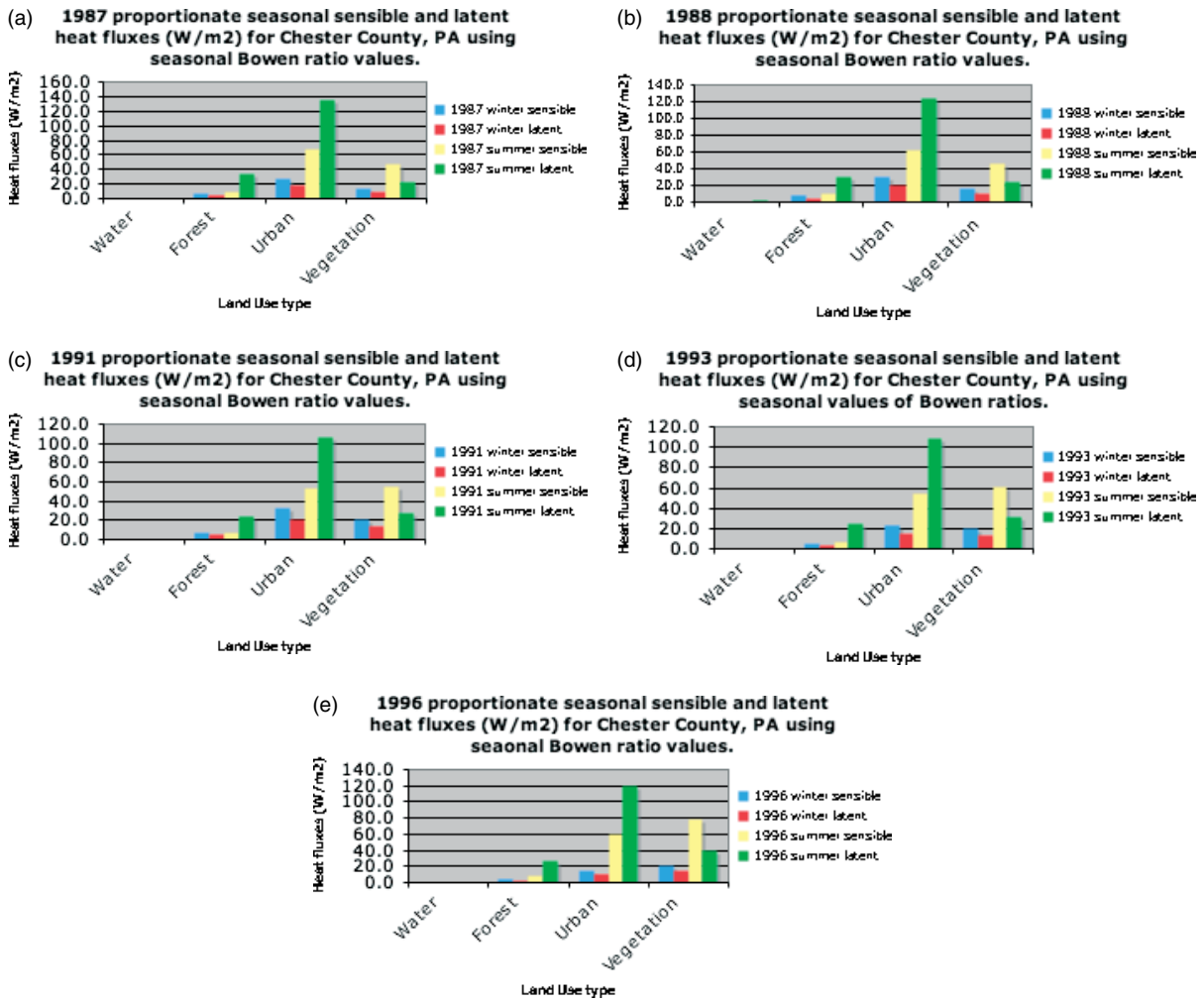

Figure 10. 1987, 1988, 1991, 1993 and 1996 proportionate seasonal sensible and latent heat fluxes (W/m2) for Chester County using seasonal Bowen ratios.

land cover types to sensible and latent heat fluxes at both the global scale and over Chester County and surroundings near Philadelphia in Pennsylvania, USA.

The sensible and latent heat fluxes at the global scale were computed as follows

- The total net radiation was first estimated from radiative transfer theory. Remotely observed values were also used to repeat the calculations.
- The annual ground heat flux ≈ 0
- The sensible and latent heat fluxes were computed by simultaneously solving the energy balance and Bowen ratio equations.
- The proportionate sensible and latent heat fluxes due to each land cover type were obtained by multiplying the computed fluxes by the fraction of the Earth covered by that particular land cover type.

Comparing the contributions from the different land cover types (water, forest, vegetation, desert and urban) to the sensible and latent heat fluxes, urban land cover has the least impact on the global climate. A realistic representation of urban land cover in global climate models may not be crucial at this time. However, the calculations confirm that the current method of representing the different fractions of the different land cover types within a grid cell is important. For example, using empirical data at the global scale, deserts gave the largest sensible heat while water gave the largest latent heat flux. However, vegetation land cover gave the largest proportionate sensible and latent heat fluxes. The same results were obtained for the five different years studied using the remotely observed data. This indicates that the approach that uses the estimates of surface total radiation from radiative transfer theory can be relied upon for certain inferences.

The sensible and latent heat fluxes at the regional scale (Chester County, PA) were computed as follows

- The values of the monthly total net radiation was obtained for a $1^\circ \times 1^\circ$ grid box with centre coordinates of 39.5^oN and 75.5^oW from the NASA GEWEX SRB data product
- An estimate of the anthropogenic heat flux was obtained from the diurnal and seasonal heating profile for Philadelphia (e.g. Sailor and Lu, 2004).
- The ground heat flux was computed as a percentage of the net radiation. The percentage is different for

DOI: 10.1002/joc

different times of the day (10% during daytime and 50% during nighttime) (e.g. Wallace and Hobbs, 2005; Liebethal and Foken, 2007). So an average of the two percentages (i.e. 30%) was used in the calculation
- The sensible and latent heat fluxes due to urban land cover were computed by simultaneously solving the surface energy balance equation for urban landscape (Equation 4) and the Bowen ratio equation
- The sensible and latent heat fluxes due to the other land cover types (i.e. water, forest and vegetation) were computed by simultaneously solving the surface energy balance equation (Equation 4) and the Bowen ratio equation
- The proportionate heat flux (sensible or latent) due to each land cover type was obtained by multiplying the heat flux by the fractional cover of that land cover type.

It has been shown from an analytical approach that the impact of urbanization is important at the regional scale. The impact of urban land cover becomes relatively more important as the fraction of urban land cover increases. This can be seen by comparing the 1987, 1988, 1991, 1993 and 1996 turbulent flux values in Figure 8.

The analytical method in this study can be used to estimate the relative importance of the impact of urbanization over any region on the globe, once the critical data needed are available. The critical data needed are the seasonal total net radiation (which will become available to the general public in the near future from the NASA project), the fraction of each land cover type in the region and an estimate of the anthropogenic heat flux. For studies over the USA, anthropogenic heat profiles can be estimated from the work of Sailor and Lu (2004).

Appendix

A. Global net radiation

The solar constant, or solar parameter S_0, or total solar irradiance (e.g. Glickman, 2000), is the flux density of solar radiation at the outer boundary of the Earth's atmosphere that is received on a surface held perpendicular to the Sun's direction at the mean distance between the Earth and the Sun.

The solar constant is less if

- the Earth were at a distance greater than the mean Earth–Sun distance (or vice versa)
- the receiving surface was other than perpendicular to the solar beam
- the measurement were made within the atmosphere or at the Earth's surface, because some radiation was depleted by absorption and backscattering to space

(e.g. Griffiths and Driscoll, 1982).

Mathematically, S_0 is the ratio of the total emission from the Sun, 3.865×10^{26} W, and the area of an imaginary sphere surrounding the Sun. If the mean distance between the Earth and the Sun is 1.5×10^{11} m, then

$$S_0 = \frac{3.865x10^{26}W}{4\pi(1.5 \times 10^{11}m)^2} = 1367Wm^{-2} \qquad (10)$$

(e.g. Aguado and Burt, 2001)

The total amount of solar radiation intercepted by the Earth is S_0 times the area over which this radiation is absorbed. The Earth appears like a disk to the Sun, and the area of this disk is the intercept area. Thus, total area $= S_0\pi r^2$, where r is the mean radius of the Earth (6.37×10^6 m),

This amount of radiation is spread unequally over the Earth's surface, an area four times as great as the intercept area. This is because the surface area of a sphere is four times its cross sectional area (or area of a sphere is four times that of a circle of the same diameter). Thus, the average amount of solar radiation available at the top of the atmosphere, per unit area and time, is

$$\frac{S_0}{4} = 340 \text{ Wm}^{-2}. \qquad (11)$$

Using the Earth's albedo of 0.3 implies that 30% of this amount is reflected, and thus, 70% is absorbed. So the actual amount of available solar radiation is

$$0.70 \times 340 = 238 \text{ Wm}^{-2} \qquad (12)$$

This is the flux density of radiation which must be emitted if the Earth emits to space as much radiation as it receives from the Sun.

The surface is radiatively heated with a net gain of energy of 30% of the solar incoming energy, while the atmosphere loses the same 30% of energy and is radiatively cooled. That is, for the total radiation, the atmosphere loses 30%, which is gained by the surface. This imbalance is compensated by a transfer of energy from the ground to the atmosphere in the form of sensible heat (about 4%) and latent heat (about 26%) (e.g. Lenoble, 2001).

The global radiation budget for short waves is that 30% of the incoming radiation is reflected at the top of the atmosphere, 20% is absorbed by the atmosphere and 50% is absorbed by the ground. The budget for the long waves is 70% is emitted at the top of the atmosphere, 50% is lost by the atmosphere and 20% is lost by the ground (e.g. Lenoble, 2001).

Thus, the mean surface solar irradiance is 50% of 340 Wm^{-2} which is 170 Wm^{-2}. That is, half the incoming solar radiation penetrates the clouds and greenhouse gases to the Earth's surface. These gases and clouds re-radiate most of the absorbed energy back down toward the surface. This is the mechanism of the greenhouse effect.

In summary:

- The surface gains a total net radiation of about 100 Wm^{-2} globally. The total net radiation is the difference between the net solar radiation of about 170 Wm^{-2}

DOI: 10.1002/joc

and the net IR radiation of about 60 Wm^{-2}. The net IR radiation was computed using a surface temperature of 15 ^{0}C (i.e. observed global mean surface temperature) and recalling that

$$T_a = 0.85^* T_s \tag{13}$$

where T_a is the temperature of the atmosphere and T_s is the surface temperature. Thus, a net upward IR irradiance of 390 Wm^{-2} and a net downward IR irradiance of 330 Wm^{-2} were obtained. That is,

Let surface temperature $T_S \approx 15\ ^oC$. Thus, emitted radiation, $\sigma T_S^4 \approx 390\ \ Wm^{-2}$ where $\sigma = 5.67 \times 10^{-8}$ $Wm^{-2}\ K^{-4}$ is Stefan-Boltzmann's constant.

Thus, upward IR irradiance is approximately 390 Wm^{-2}. Downward IR irradiance at the surface $\approx 0.85\ \sigma\ T_S^4 \approx 330\ Wm^{-2}$

- Irradiance reaching the Earth from the Sun is

$$S_0 = \sigma T_{sun}^4 (\frac{r_{sun}}{r_d})^2 Wm^{-2} \tag{14}$$

where r_d is the radius of the sphere energy spreads over between the Sun and Earth (and this is equal to the mean Sun-Earth distance).

References

Aguado E, Burt JE. 2001. *Understanding Weather and Climate* (2nd edn). Prentice Hall: New Jersey, 505 pp.

Arthur ST, Carlson TN, Ripley DAJ. 2000. Land use dynamics of Chester County, Pennsylvania, from a satellite remote sensing perspective. *Geocarto International* **15**(1): 25–35.

Arnfield AJ. 2003. Two decades of urban climate research: a review of turbulence, exchanges of energy and water, and the urban heat island. *International Journal of Climatology* **23**: 1–26.

Bornstein R. 1987. *Mean Diurnal Circulation and Thermodynamic Evolution of Urban Boundary Layers*, from Modeling the Urban Boundary Layer. American Meteorological Society: Boston; 52–93.

Bottyan Z, Kircsi A, Szegedi S, Unger J. 2005. The relationship between built-up areas and the spatial development of the mean maximum urban heat island in Debrecan, Hungary *International Journal of Climatology* **25**: 405–418.

Brown MJ. 2001. Urban parameterizations for mesoscale meteorological models, in *Mesoscale Atmospheric Dispersion*, LA-UR-99-5329, Boybeyi Z (ed). WIT Press: Southampton; 193–255.

Carlson TN, Arthur ST. 2000. The impact of land use - land cover changes due to urbanization on surface microclimate and hydrology: a satellite perspective. *Global and Planetary Change* **25**: 49–65.

Chase TN, Pielke RA, Kittel TGF, Nemani R, Running SW. 2000. Simulated impacts of historical land cover changes on global climate in northern winter. *Climate Dynamics* **16**: 93–105.

Gao F, Schaaf CB, Strahler AH, Roesch A, Lucht W, Dickinson R. 2005. MODIS bidirectional reflectance distribution function and albedo Climate Modeling Grid products and the variability of albedo for major global vegetation types *Journal of Geophysical Research* **110**: D01104, DOI 10.1029/2004JD005190.

Glickman T (ed). 2000. *Glossary of Meteorology*, (2nd ed). American Meterological Society: Cambridge, Massachusetts; 855.

Hebble EE, Carlson TN, Daniel K. 2001. Impervious surface area and residential housing density: a satellite perspective. *Geocarto International* **16**(1): 13–18.

Griffiths JF, Driscoll DM. 1982. *Survey of Climatology*, Charles E (ed). Merrill Publishing Company: Columbus; 358.

Land Area Classification by Ecosystem Type. 2003. http://earthtrends.wri.org/datatables/index.php?theme=9.

National Aeronautics and Space Administration Global Energy and Water Cycle Experiment Surface Radiation Budget. http://gewex-srb.larc.nasa.gov/.

Land Processes Distributed Active Archive Center. http://lpdaac.usgs.gov/modis/mcd43c3v4.asp.

IPCC. 2007. Climate Change 2007, in *The Physical Science Basis. Contribution of the Working Group 1 to the Fourth Assessment Report of the Intergovernmental Panel on Climate Change*, Solomon S, Qin D, Manning M, Chen Z, Marquis M, Averyt KB, Tignor M, Miller HL (eds). Cambridge University Press: Cambridge, New York.

Jiang X, Wiedinmyer C, Chen F, Yang Z-L, Lo JC-F. 2008. Predicted impacts of climate and land use change on surface ozone in the Houston, Texas area. *Journal of Geophysical Research* **113**: D20312.

Jin M, Shepherd JM. 2005. Inclusion of urban landscape in a climate model. How can satellite data help? *Bulletin of the American Meteorological Society* **86**(5): 681–689.

Jin M, Shepherd JM, Peters-Lidard C. 2008. Development of a parameterization for simulating the urban temperature hazard using satellite observations in climate model. *Nature Hazards* **43**: 257–271.

Karl TR, Diaz HF, Kukla G. 1988. Urbanization: its detection and effect in the United States climate record. *Journal of Climatology* **1**(11): 1099–1123.

Kiehl JT, Trenberth KE. 1997. Earth's annual global mean energy budget. *Bulletin of the American Meteorological Society* **78**(2): 197–204.

Lamptey BL, Barron EJ, Pollard D. 2005a. Simulation of the relative impact of land cover and carbon dioxide to climate change from 1700 to 2100. *Journal of Geophysical Research* **110**: D20103.

Lamptey BL, Barron EJ, Pollard D. 2005b. The Impact of agriculture and urbanization on the climate of the Northeastern United States. *Global and Planetary Change* **49**: 203–221.

Lenoble J. 2001. *Atmospheric Radiative Transfer*. Deepak Publishing: Virginia.

Liebethal C, Foken T. 2007. Evaluation of six parameterization approaches for the ground heat flux. *Theoretical and Applied Climatology* **88**: 43–56.

Lin C-Y, Fei Chen JC, Huang W-C, Chen Y-A, Liou W-N, Chen S-C, Liu. 2008. Urban heat island effect and its impact on boundary layer development and land-sea circulation over northern Taiwan. *Atmospheric Environment* **42**: 5635–5649.

Miao S, Chen F, LeMone MA, Tewari M, Li Q, Wang Y. 2008. An observational and modeling study of characteristics of urban heat island and boundary layer structures in Beijing. *Journal of Applied Meteorology and Climatology* (Submitted).

Masson V. 2006. Urban surface modeling and the meso-scale impact of cities. *Theoretical and Applied Climatology* **84**: 35–45.

Miller G, Mangan J, Pollard D, Thompson S, Felzer B, Magee J. 2005. Sensitivity of the Australian Monsoon to insolation and vegetation: implications for human impact on continental soil moisture balance. *Geology* **33**(1): 65–68.

Molders N, Olson MA. 2004. Impact of urban effects on precipitation in high latitudes. *Journal of Hydrometeorology* **5**(3): 409–429.

Oke TR. 1987. *Boundary Layer Climates* (2nd ed). University Press: Cambridge; 435.

Oke TR. 1982. The energetic basis of the urban heat island. *Quarterly Journal of the Royal Meteorological Society* **108**(455): 1–24.

Paumier JO, Brode RW. 2004. User's Guide for the American Meteorological Society/Environmental Protection Agency Air Quality Regulatory Model (AERMOD) Meteorological Preprocessor (AERMET). EPA-454/B-03-002, 252.

Sailor DJ, Lu L. 2004. A top-down methodology for developing diurnal and seasonal anthropogenic heating profiles for urban areas. *Atmospheric Environment* **38**: 2737–2748.

Schaaf CB, Gao F, Strahler AH, Lucht W, Lia X, Tsanga T, Strugnella NC, Zhanga X, Jina Y, Mullerc JP, Lewisd P, Barnsleye M, Hobsone P, Disneyd M, Robertsd G, Dunderdalec M, Dollc C, d'Entremontf RP, Hug B, Liangh S, Privette JL, Roy D. 2002. First operational BRDF, albedo nadir reflectance products from MODIS. *Remote Sensing of Environment* **83**: 135–148.

Shepherd JM, Jin M-Y. 2004. Linkages between the built urban environment and earth's climate system. *EOS* **85**(23): 227–228.

Trusilova K, Jung M, Churkina G, Karstens U, Heimann M, Claussen M. 2008. Urbanization impacts on the climate in Europe: numerical experiments by the PSU-NCAR Mesoscale Model (MM5). *Journal of Applied Meteorology and Climatology* **47**(5): 1442–1455.

Voldoire A, Royer JF. 2004. Tropical deforestation and climate variability. *Climate Dynamics* **22**: 857–874.

Wallace JM, Hobbs PV. 2005. Atmospheric Science. *An Introductory Survey* (2nd ed). Academic Press: Amsterdam; 483.